Influence of pressure on the PD and induced aging behavior of polyimide insulation under repetitive pulse voltage

Zheng, Changjiang; Wang, Qian ; Shen, Zhan; Bak, Claus Leth; Silva, Filipe Miguel Faria da; Wang, Huai

Published in:
IEEE Transactions on Dielectrics and Electrical Insulation

DOI (link to publication from Publisher):
10.1109/TDEI.2023.3236595

Publication date:
2023

Document Version
Accepted author manuscript, peer reviewed version

Influence of pressure on the PD and induced aging behavior of polyimide insulation under repetitive pulse voltage

Changjiang. Zheng, Qian Wang, Zhan Shen, Claus Leth Bak, Filipe Faria da Silva and Huai Wang

***Abstract*—Reduction of air pressure can influence insulation material's behavior with respect to resisting partial discharge (PD) generation and its induced aging process. This may bring threat to the insulation reliability of medium frequency transformers working under low pressure condition, considering they are exposed to high probability of PD inception caused by PWM voltage. Aiming at investigating the performance of insulation of medium frequency transformer being operated in an environment with a decreasing pressure, this paper introduces a test system that can conduct partial discharge and endurance lifetime tests under repetitive pulse voltage and controlled pressure. Using this test system and focusing on polyimide film, which is one of the main insulation materials used by medium frequency transformers, partial discharge and endurance lifetime tests are conducted under different pressures. The results show that partial discharge inception voltage decreases with decreasing pressure. However, the changing of partial discharge magnitude, time lag and its induced insulation lifetime do not change monotonously. Surface of the failed insulation samples show that the erosion area caused by partial discharge is larger under lower pressure. The mechanisms behind the changing of partial discharge time lag, discharge magnitude, endurance lifetime, along with the discharge eroded area with pressure are discussed in detail.**

***Index Terms*— Medium frequency transformer, partial discharge (PD), Low pressure, polyimide, Insulation aging**

I. INTRODUCTION

In many modern power electronic systems, transformers are necessary for voltage scaling up/down and electrical isolation. These transformers are usually called medium frequency transformer for they usually work with PWM voltage with frequency higher than 50/60 Hz power frequency [1]. With this higher working frequency, the core of the transformer can reach smaller size, which gives rise to lower manufacturing costs. Also, combined with power electronic switches, medium frequency transformers have higher controllability. Because of these advantages, medium frequency transformers are widely used in modern power electronic applications, such as railway traction, DC grids, etc.

Working under PWM voltage with short rise time, overvoltage can be induced in the winding of the electrical devices such as motors and transformers and the probability of partial discharge (PD) inception would be higher. Continuous PD can degrade the insulation material quickly and lead to premature breakdown [2].

Studies on the insulation failure mechanism under continuous PDs show that environment factors can affect the PD behavior and its aging speed on the insulation [3]. Among these factors, pressure is very important. According to the Paschen Curve in Fig. 1, if the distance of the air gap remains the same, before reaching the critical point (minimum breakdown strength), breakdown strength of gaseous dielectrics will be reduced with the reduction of pressure [4]. Paschen curve is obtained under uniform electric field. Yet, whether the field is uniform or not, the influence of reducing air density on the air's dielectric strength is still the same. Therefore, similar phenomenon can be expected also under non-uniform filed. For solid insulation with air ducts as defects, the change of breakdown strength of air can directly affect its insulation reliability to resist PD inception. In addition, the reducing of gas density can also affect the mean free path of charge (or electron), which can in turn affect the discharge intensity.

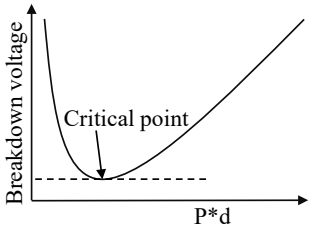

Fig. 1. Paschen Curve

(a)

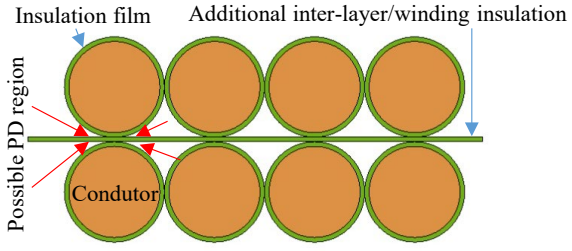

(b)

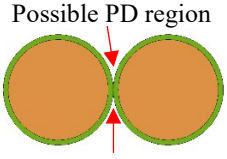

Fig. 2. Possible PD region in the winding of the transformer: (a) With additional inter layer/winding insulation. (b) Without additional inter layer

insulation.

For medium frequency transformers, the effect of pressure is a practical problem. Some medium frequency transformers are working in high-altitude area and recently aircrafts are relying more on power electronic systems in which transformers are usually applied [5]. Besides, unlike the conventional transformer that usually use oil-paper insulation, medium frequency transformers usually use dry-type insulation. Thus, air ducts may exist between adjacent winding layers or adjacent windings where lies a high voltage drop and are more likely to be the source of PD. One of the examples can be seen in Fig. 2(a), the conductors of the upper side and down side may belong to adjacent layers of a winding or belong to different windings. Strong electric field due to high voltage drop and dielectric refraction would concentrate on the places where the red arrows point at, leading to a PD that can erode the surface of the insulation film. For the sake of a compact design, some of the medium frequency transformer may not apply an additional inter-layer insulation. If the gap between the conductors of adjacent winding layers is not enough like in Fig. 2(b), PD is more likely to be triggered and cause greater threat to the insulation film that directly covers the conductor. If the pressure goes lower in these abovementioned air ducts, the probability of PD inception may be even greater.

Previous studies focusing on pressure's effects on PD behavior and its induced aging process provide some information and reference for the future insulation studies in the field of medium frequency transformer. In [3], the author finds lower pressure give rise to lower PDIV and shorter lifetime with presence of PD. Under high pressure, before the breakdown, PD energy shows larger variety along with the aging than that under low pressure. In [6], PDIV tests are conducted on the voids in epoxy. The author finds that with the size of void fixed, for the P*d around the critical point of Paschen curve (alike depicted in Fig. 1), the test result is usually higher than the calculated one. This may be due to the reason that under these low pressures, when the voltage magnitude reaches the calculated PDIV, the PD intensity is too weak (well below the noise) to be detected by the traditional current sensor [7]. Higher voltage magnitude is needed to generate PDs strong enough to be detected, which leads to an unprecise result. Authors in [7] also analyze the PD light waveform and find that when the pressure goes below 260 Pa, the rise time of the PD waveform increases obviously. They propose the speculation that PD type changes from streamer discharge into Townsend discharge when pressure goes extremely low. In [8], the authors conduct PD experiments on gas dielectrics including air, He and Ar. Under non-uniform electric field provided by different electrode types, the shapes of PDIV-pressure curves under different gas dielectrics all agree well with the Paschen Curve. Larger PD glow can be observed under lower pressure, which indicate that PD volume expands with the decreasing of pressure. Literature [9] measures the space charge density during the corona discharge under different pressures. Results show that, more space charge would be produced under lower pressure. Since stronger discharge causes stronger ionization and creates more space charge, the author believes that low pressure can give rise to stronger PD intensity. Literature [10] observes the number of the PDs under extremely low pressure condition. With pressure drops from 100 Pa to 3 Pa, the number of PDs during the same time interval decreases. Literature [11] proposes comparative simulations of PD features under one atmosphere pressure (1 atm) and a half atmosphere pressure (0.5 atm). With 0.5 atm, although the individual PD intensity is weaker than that under 1 atm, the occurrence rate of PD is doubled. This makes the total amount of charge per cycle under 0.5 atm obviously larger than that under 1 atm. Literature [12] conducts PD aging tests on the PCB board under different pressures. It finds that growth rate of silicon coating surface crack due to PD erosion is obviously faster under lower pressures.

Since changing of PD features with pressure can affect the accuracy of PD monitoring and the long term reliability of different kinds of insulation, these above-mentioned studies remind the field of medium frequency transformers of the necessity to pay attention to the influence of the pressure. However, studies in [3, 6-12] are conducted using traditional power frequency sinusoidal voltage or DC voltage, of which the frequency and voltage rise time is very different from that of PWM voltage. With different voltage parameters, the influence of pressure on the PD feature (including the magnitude and phase distribution) may also be different [13]. Comparative studies between PWM voltage and sinusoidal voltage are conducted in [14]. Under sinusoidal voltage, with pressure decreasing, the main energy distribution of PD signal would shift to lower frequency range. While under PWM voltage, PD energy distribution in frequency domain shows no obvious change with decreasing pressure. Therefore, conclusions from the studies using AC sinusoidal voltage or DC voltage cannot be used directly for studies on the insulation working under PWM-like pulse voltage.

There are a few research regarding effects of pressure on PD behaviors induced by pulse voltage. Literature [15] proposes PD inception tests under different pressures using pulse voltage and find that with lower pressure, repetitive PDs can be generated with lower voltage magnitude. In [16], a FEM model is proposed to simulate the PD characteristics under pulse voltage and different pressures. According to the simulation results, with the decreasing of the pressure, longer time has to be waited for the PD inception, while PD duration time and PD true charge are both higher under lower pressures. The study object is the cavity in the silicone gel used for the IGBT/MOSFET module's package. Although its geometric and dielectric properties are quite different from the insulation of transformers, the study indicates a stronger PD erosion when pressure is lower, which should not be ignored for the insulation design of other electrical devices. In [17], PD studies on the trench of PCB board under different pressures are conducted under unipolar pulse voltage. Both PD magnitude and number of PDs per minute become larger when pressure decreases. This trending keeps the same whether the pulse voltage is positive or negative. These literatures remind the possibility of greater PD threat under lower pressure for other electrical devices like

medium frequency transformer working under PWM-like voltage and necessity of more studies. For the first step, systematic investigation on pressure's effect on the insulation material that is usually applied in medium frequency transformers is needed.

This paper builds a test system with abilities to generate repetitive pulse voltage, conduct PD detection and create low pressure condition. Based on this system, under different pressures, PD and endurance lifetime tests on the polyimide film, which is usually used for the insulation of medium frequency transformer [18], are conducted. Change trending of the PD inception, PD features and endurance lifetime with pressure drops from 1 Bar to 0.3 Bar are shown and the mechanism for the results are discussed in detail. These above results reveal that polyimide film suffers from greater risk of PD inception and deterioration when pressure decreases within the above mentioned range, which indicates the necessity of similar studies on the whole medium frequency transformer prototype or transformer related insulation structures.

II. EXPERIMENT SETUP

To investigate the influence of pressure on the medium frequency transformer's insulation reliability, PD and endurance lifetime tests on the insulation sample under different pressures should be conducted. To realize these experiments, a test system is needed. This system should be able to generate repetitive pulse voltage and create low pressure circumstances (since this study focuses on the PD and its aging process on insulation working under high-altitude area or aircrafts, the pressure higher than sea level pressure is not considered) and detect PD with high accuracy. This section introduces the test system and experiment parameters in detail.

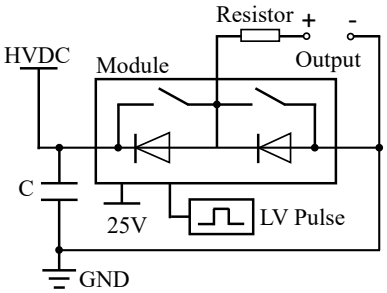

Fig. 3. Pulse voltage generator based on a half bridge power electronic power module

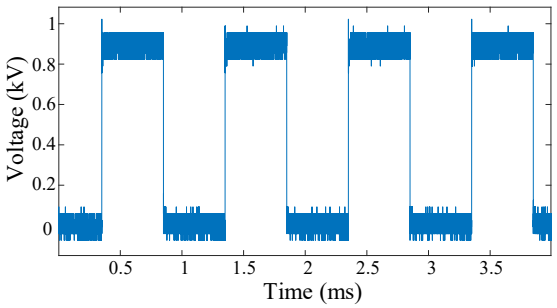

Fig. 4. Repetitive pulse volage waveform with 1 kV peak value and 1 kHz frequency

A. PULSE VOLTAGE GENERATOR

To conduct PD and aging studies, a voltage generator is needed to generate a pulse voltage that can simulate the medium frequency and short rise time of the PWM voltage. In this paper, a pulse voltage generator is built based on a half-bridge power electronic module. Seen in Fig. 3, a HVDC source is applied as high voltage input, while a capacitor is used for DC voltage stabilization. The resistor is used for regulating the pulse voltage rise time and restricting the output current to prevent the module from overheating. The half bridge module is powered by a 25 V DC source and triggered by a 5 V pulse generator. This generator can produce repetitive unipolar pulse voltage. A typical output waveform of this pulse voltage generator can be seen in Fig. 4.

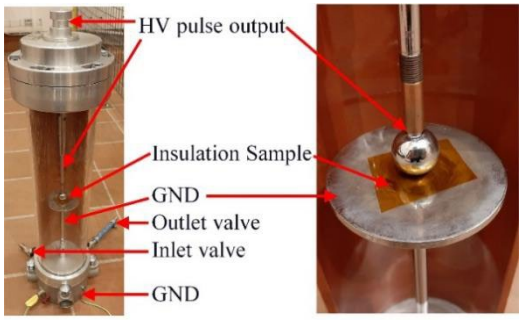

Fig. 5. Pressure tank and the electrodes inside

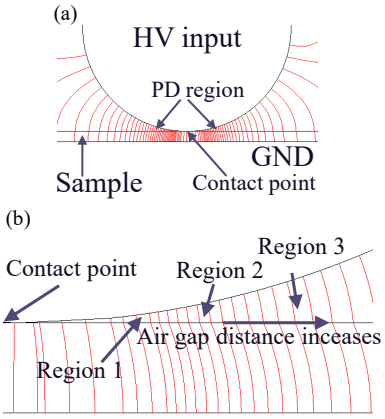

Fig. 6. Electric field distribution of the sphere-plate electrode: (a) Overall electric field distribution; (b) Zoom in of the air duct close to the contact point

B. PRESSURE CONTROLLING

A pressure tank seen in Fig. 5 is used to control the pressure for the experiments. By pumping out gas through the outlet valve, it can change the pressure inside from 1 Bar (corresponding to 100 kPa) to 0.3 Bar (corresponding to 30 kPa). A sphere-plate electrode is placed inside for fixing the insulation film. The sphere electrode with 20 mm diameter is added with HV output while the plate electrode with 75 mm diameter is connected to ground. When voltage is added on the insulation sample, the electric field distribution can be briefly expressed by Fig. 6. The density of lines represents the electric field intensity. It can be seen that the electric field distribution is not uniform and the air duct close to the contact point suffers from strongest electric field, where PD may be induced. This PD can break through the air duct and touch the insulation surface. As it can be seen in Fig. 6(b), dielectric refraction would happen in the interface between the air and the insulation film, which changes the direction of the lines and enhance the

electric field intensity in the air duct a little bit. As described in the Introduction and Fig. 2, for medium frequency transformers, PDs are likely to happen in the air duct between turns belonging to adjacent winding layers or different windings. These PDs can break through the air duct and cause erosion on the surface of insulation film. Therefore, this sphere-plate electrode is suitable for analyzing the PD behavior and its induced aging process on the insulation film used by the medium frequency transformer with the assumption that the electrical overstress already exists.

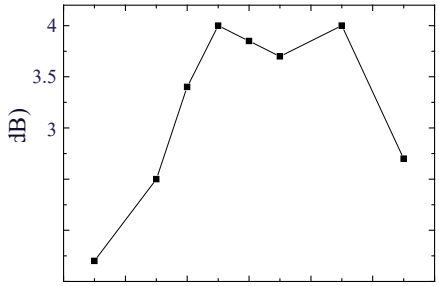

Fig. 7. Gain of the UHF antenna

C. PD DETECTION

According to studies on PD detection, under pulse voltage with short rise time (from tens of ns to several μs), strong interference would be caused by the on-off of the power electronic switches. This would make traditional detection method such as current sensor or high frequency current transducer (HFCT) unreliable to figure out the PD signal. Yet difference exists in the energy distribution in frequency domain among PD and interference signals. For the interference, most of its energy lies below 400 MHz. While for PD, its energy can spread up to more than 1.5 GHz [19]. Therefore, an Ultra-High-Frequency (UHF) antenna is the best choice for PD detection under PWM voltages. The gain of the UHF antenna used in this study is shown in Fig. 7. In frequency range from 500 MHz to 1.5 GHz, its gain is more than 2 dB. To further reduce the interference, a 400 MHz – 3 GHz band-pass filter is connected to the antenna's output interface. The waveform detected by this antenna with filter is shown in Fig. 8. The magnitude of the interference has been attenuated to around 1 mV while the PD signal can be detected effectively. Since the antenna detects the electromagnetic wave signal radiated by PD, to avoid too much attenuation when it travels through the air, the antenna is placed with distance of around 8 cm from the pressure tank (seen in Fig. 9).

With these above-mentioned devices together with control and data processing unit, the test system is constructed, as shown in Fig. 10. The computer is used for controlling the HV pulse voltage generator's output voltage magnitude and frequency, and for overcurrent protection (combined with current sensor)

(a)

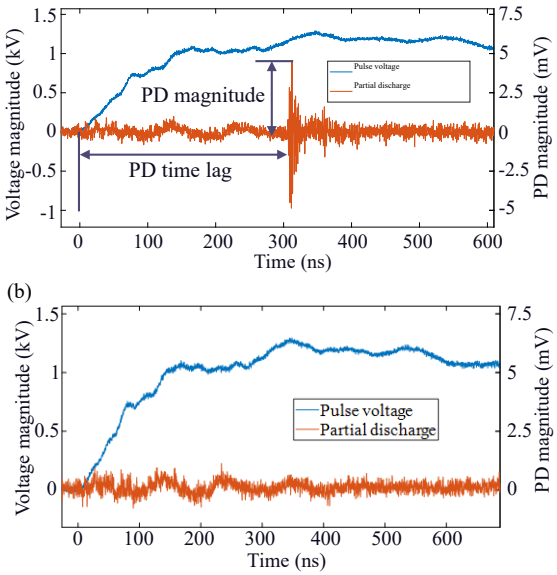

Fig. 8. Waveform detected by antenna with filter: (a) PD happens; (b) No PD happens.

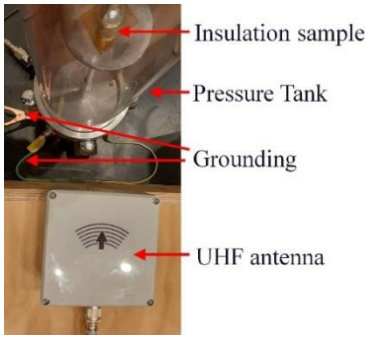

Fig. 9. UHF antenna

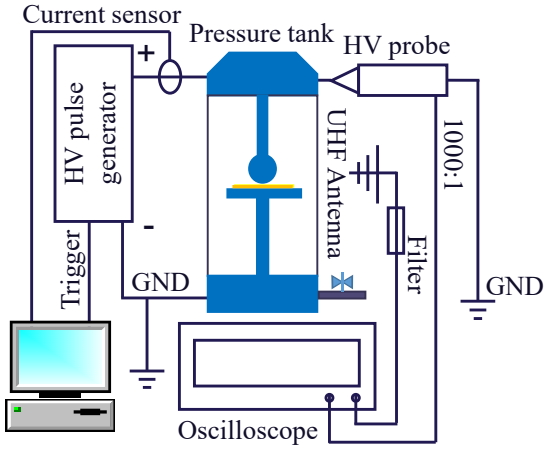

Fig. 10. Test system

D. INSULATION SPECIMEN

The insulation specimen used for the tests is the Kapton polyimide film. This insulation material is often used in the medium voltage electric devices such as motors and transformers. The thickness of the film is 0.05 mm and all the specimens for the tests are cut into square shape with 3 cm side length. Before the experiments, all specimens are cleaned by alcohol and dried in the oven for 24 hours.

E. EXPERIMENT PARAMETERS

Although overcurrent protection is available for the test system, to avoid a too high impulse current due to expected breakdown in endurance test or unexpected breakdown in other tests, the resistance of resistor in Fig. 3 is set as 1kΩ. Since the resistor is connected in serial with the insulation sample, the time constant τ of output pulse voltage would mainly be decided by the resistance and the insulation sample's capacitance, expressed as τ=RC. Because of this, the rise time of the pulse voltage is 250 ns and would be kept unchanged. Before the PD and endurance tests, PDIV test under sea level pressure is conducted in advance and the average value of the PDIV is 1.3 kV. To analyze the statistical PD features and PD's aging on insulation material, repetitive PDs should be generated during each voltage cycle, which means the voltage magnitude added on the insulation sample should be higher than PDIV. For a single transformer, although the environment condition may change, it usually works under a certain voltage rating. Considering these two factors, peak voltage value for the following PD feature and endurance tests is kept as 1.96 kV, 1.5 times the average PDIV value under sea level pressure. Different pressure values from 1 Bar to 0.3 Bar are chosen for the comparative studies. The detailed parameters for the PDIV/PD experiments are listed in Table 1. For the endurance lifetime tests, the voltage frequency is increased into 2 kHz to accelerate the aging speed while other parameters are the same as that in Table I.

Table I

PARAMETERS FOR PDIV AND PD FEATURE TESTS

Group	Rise time	Frequency	Pressure	Voltage peak value (For PD tests)
1	250 ns	1 kHz	1 Bar	1.96 kV
2			0.9 Bar	
3			0.8 Bar	
4			0.7 Bar	
5			0.6 Bar	
6			0.5 Bar	
7			0.4 Bar	
8			0.3 Bar	

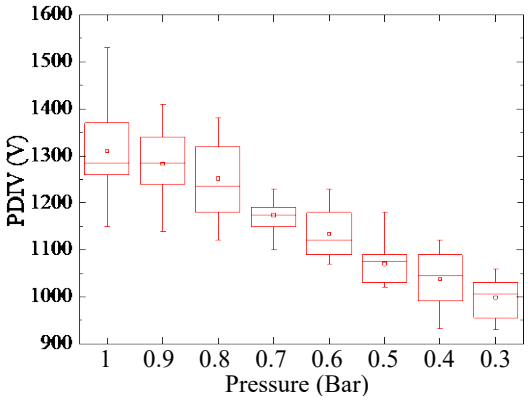

Fig. 11. PDIV under different pressures

III. EXPERIMENT RESULTS

A. PDIV EXPERIMENTS

For the PDIV tests, the oscilloscope is set as single step trigger mode, voltage magnitude is raised slowly with 10 V/s until the PD is triggered like Fig. 8(a), then the PDIV value is defined as the peak value of pulse voltage when the first PD is triggered. 5 specimens are used in each group of Table I. Then statistical PDIV values under different pressures are shown in Fig. 11. It is clear that PDIV decreases monotonously with pressure decreasing. Although for the sphere-plate electrodes, the electric field distribution in the air duct is non-uniform, the results show trending similar with Paschen's Curve that is obtained under uniform electric field.

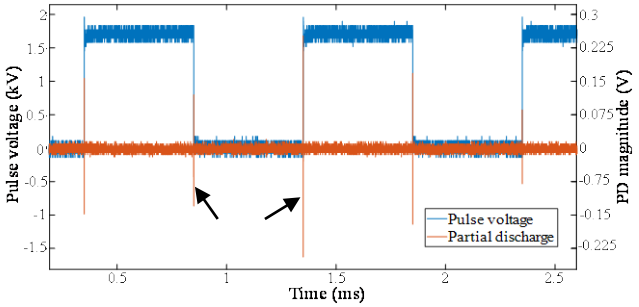

Fig. 12 PD generated by repetitive pulse voltage

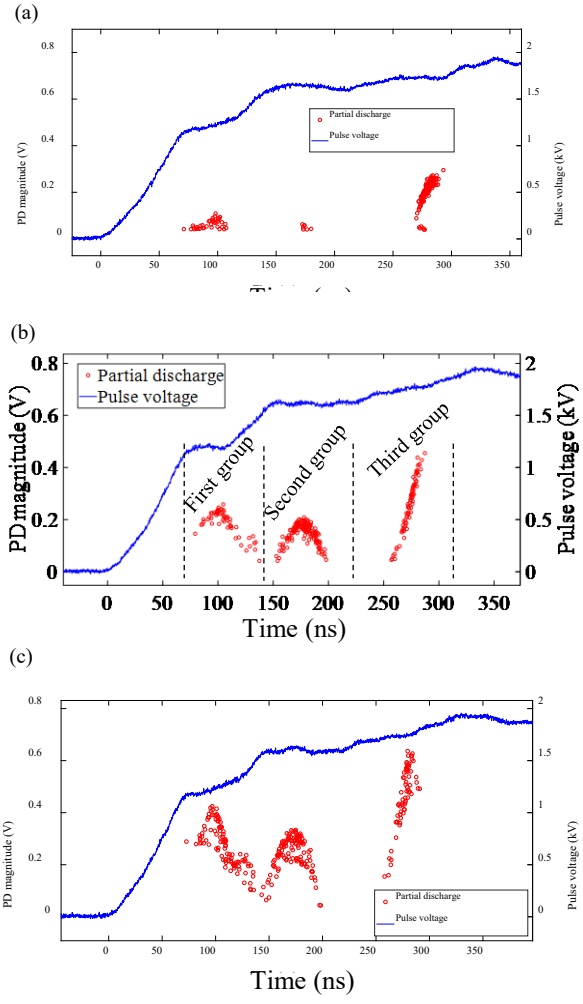

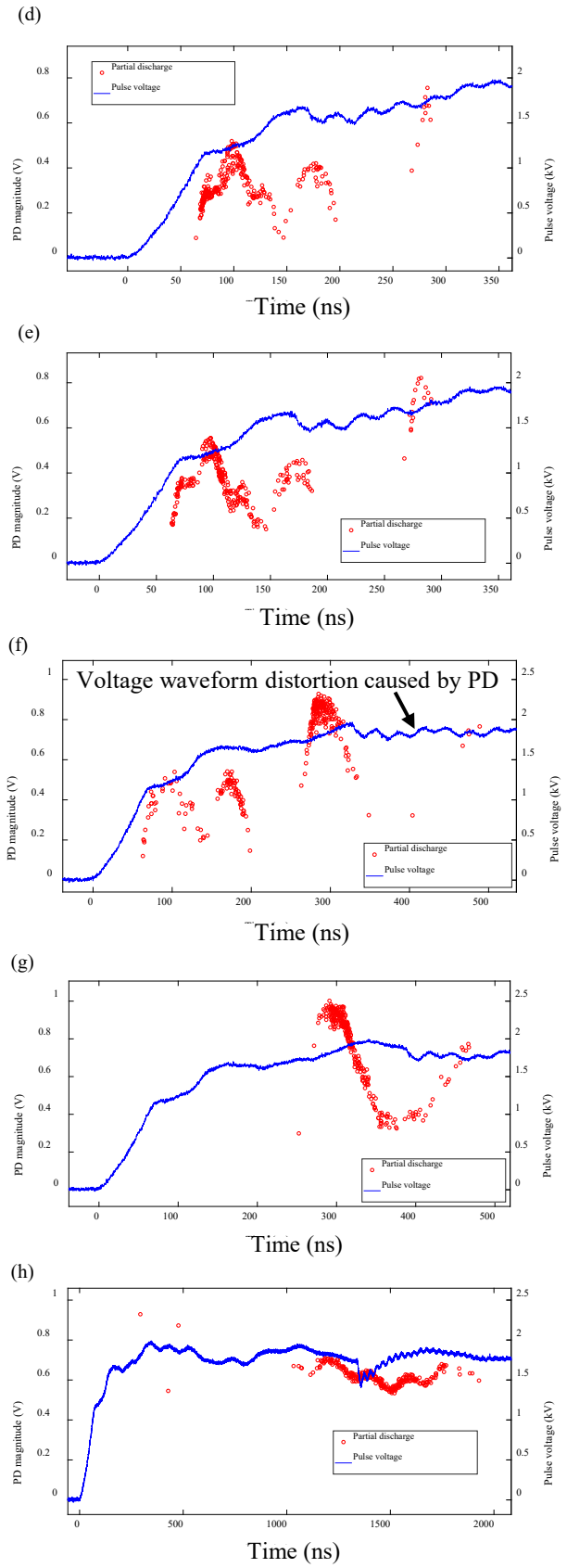

Fig. 13. Time resolved PD pattern under different pressures: (a) 1 Bar; (b) 0.9 Bar; (c) 0.8 Bar; (d) 0.7 Bar; (e) 0.6 Bar; (f) 0.5 Bar; (g) 0.4 Bar; (h) 0.3 Bar.

B. PD FEATURES

Seen as Fig. 12, PDs are generated on the rising/falling edge of the pulse voltage, or at least close to the pulse edges. No obvious PD can be found on the rest of the plateau regions of the pulse voltage. Under symmetric pulse voltage with 50% duty cycle, the statistic PD features around both the rising edge and falling edge are very similar [20]. Therefore, in the analyzing of PD feature under different pressures, we focus on the PDs generated around the rising edge. In order to get statistical PD features, 300 cycles of data are collected through the oscilloscope. Time resolved partial discharge patterns are plotted in Fig. 13. It can be seen that in most of the situations (from 1 Bar to 0.5 Bar), PDs show a similar distribution with three clusters. We divide the PDs into three groups according to which cluster they belong to as shown in Fig. 13(b). In the first group, PD happens at around 100 ns after the zero point of pulse voltage. In the second group, PD happens at around 170 ns after the zero point while the third group of PD at around 270 ns. We define the instantaneous voltage value when PD happens as PD firing voltage, then it is sure that the second group of PD has higher PD firing voltage than the first group. However, although PD magnitude shows a great variety (randomness) even under the same voltage and pressure condition, statistical PD magnitude of the second group is lower than that of the first group in most of the situation (from 1 Bar to 0.6 Bar). Apparent discharge q is one of the important factors to determine the PD intensity [21]. For analyzing the PD that bridges air duct between the sphere electrode and the insulation surface in our experiments, we can regard the air duct as a capacitor and estimate the q through Equation (1).

$$q = C \cdot V_c = C \cdot h \cdot f \cdot E_i \qquad (1)$$

Where V_c is the applied voltage value when PD happens, C is the capacitance of air duct, h is the height of the air duct. While f is field enhancement factor. In the region that PD is possible to be triggered, voltage is added between two dielectrics, air and polyimide. Since permittivity of polyimide is much higher than that of air, an enhancement of electric field is present in the air duct [4]. Notice that in Fig. 6, the air duct height is not constant from the contact point to outer area. Also, the bottom side of the air duct is not contacted with the metal plate electrode but with the insulation film. These factors make the values of C and f difficult to be determined. So (1) can only be used for a rough estimation. The total electric field strength E_i can be expressed as E_a-E_q, where E_a is the applied electric field and E_q is the electric field produced by surface charge, which usually has polarity opposite to E_a.

Seen in Fig. 6, starting from the contact point, if the distance goes longer, the air duct length d is also longer. This means under the same added voltage, the electric field intensity is lower according to E=U/d. Therefore, higher added voltage amplitude is needed for longer air duct to meet breakdown. Then the PD situation can be analyzed approximately by simply dividing the air duct into three regions shown in Fig. 6(b). This separation is based on breakdown voltage of air duct (corresponds to partial discharge inception field E_{pdiv} multiplied by d). For region 1, the breakdown voltage is lower than 1.58

kV. For region 2, the breakdown voltage lies from 1.58 kV to 1.7 kV. For region 3, the breakdown voltage is higher than 1.7 kV. These breakdown voltage value ranges cover the ranges of PD firing voltages in the three PD groups (seen from Fig. 14) respectively. Notice that, after the electric field intensity of air duct exceeds the E_{pdiv}, for triggering the PD, there is a time delay Δt to be waited for the presence of initial electron (this process is not affected by pressure) and the forming of electron avalanche. This factor may make the E_i when PD happens different from E_{pdiv}. And the decreasing of pressure can make the time for forming the electron avalanche longer (this would be discussed in detail in section IV). Yet, in relatively high pressure range (higher than 0.4 Bar), the total Δt would not be very long, the practical breakdown voltage of these three air duct regions lies within the above-mentioned breakdown voltage value ranges correspondingly. During the pulse voltage rising edge, the electric field of region 1 would exceed the partial discharge inception field E_{pdiv} at first. This mainly contributes to the first group of PD. When the voltage instantaneous value continuous to increase to more than 1.58 kV (150 ns from the zero point), the E-field in region 2 can reach the E_{pdiv} and triggers PD mainly in the second group. Due to stray parameters of the power electronic modules and the resistor in Fig. 3, the rising edge of the pulse voltage is not a smooth curve. Zoom-in of the pulse voltage rising edge is shown in Fig. 14. For the PD happens in region 1, during Δt, the voltage keeps rapid rising and give rise to a higher E_i when PD is triggered. While for the second group of PD happens in region 2, during Δt, the voltage shows no obvious increasing and even drops a little bit, which give rise to a relatively lower E_i. This is the reason why second group of PD usually has lower magnitude compared to that of first group. When the voltage further rises to exceed the E_{pdiv} of region 3, the PDs of this region that mainly form the PDs in the third group can be triggered. Seen from Fig. 14, in this time range, voltage also keeps rising, and due to a longer air gap distance, longer time delay Δt is needed for forming the electron avalanche. These factors make E_i higher when the third group of PD happens and give rise to stronger PD intensity. It should be noticed that, although the situation of PDs in the three regions of Fig. 6(b) mainly contributes to the PD pattern shown in Fig. 13 from 0.9 Bar to 0.5 Bar, it does not mean that the PDs in these three regions fully correspond to the PD groups in Fig. 14. A typical exception can be found in Fig. 13(a). With 1 Bar pressure, the PDIV is highest, while we conduct all the PD feature tests under the same 1.96 kV peak voltage value. This means under 1 Bar, the overvoltage compared to the PDIV is relatively lowest. This may lead to a result that less PD can happen in the first group (in the time region of first group in Fig. 14, pulse voltage instantaneous value is not very large) even in region 1 while more PDs on the third group. In this situation, the PD in the third group would not only be the PD happens in region 3, but also in region 2 and region 1.

Taking one of the regions of the air duct in Fig. 6(b) as an example, the change of the electric field strength is similar with that proposed in [2] and can be expressed by Fig. 15. At first, the E_i increases along with the rising edge of the applied electric field E_a and exceeds E_{pdiv}. After the generation of initial electron, the PD happens. Then a large amount of surface charge deposit on the insulation surface, which formed E_q with an opposite direction to E_i. Thus, E_i is reduced to $E_{res1}= E_a-E_q$ that is smaller than E_{pdiv}. Afterwards, the applied E_a reaches the plateau region and stops increasing. Although due to the insulation material's surface conductivity, some of the surface charge would be dissipated, it would not be enough for the E_i to exceed the E_{pdiv} again before meeting the falling edge. When the E_a meets the falling edge, E_q is still very strong. The absolute value of $E_i= E_a-E_q$ reaches a high value and exceeds the E_{pdiv} in an opposite polarity. Then, another PD happens and E_i decreases into E_{res2}. When the next cycle of pulse voltage comes, the above-mentioned process repeats. This is why PDs are mainly incepted around the rising/falling edge.

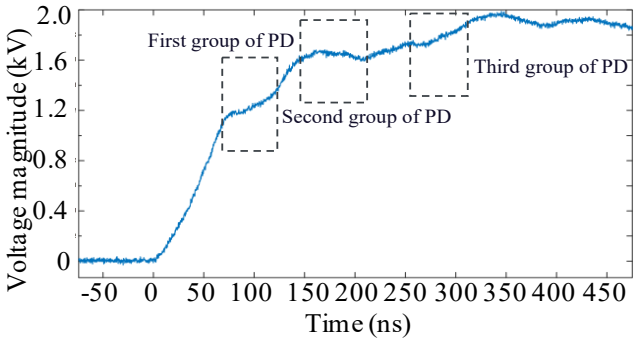

Fig. 14. Zoom in of rising edge of the pulse voltage

To show the changing of statistical PD magnitude and time lag more directly, box-charts of PD magnitude and PD time lag are plotted in Fig. 16 and Fig. 17 respectively. Note: the definitions of PD magnitude and time lag are shown in Fig. 8 (a). We can see that PD magnitude increases with pressure decreases from 1 Bar to 0.4 Bar. Yet, when pressure drops from 0.4 Bar to 0.3 Bar, PD magnitude decreases. When air pressure is larger than 0.7 Bar, PD time lag decreases with pressure decreasing. When pressure is lower than 0.7 Bar, PD time lag increases with pressure decreasing. When pressure change from 0.4 Bar to 0.3 Bar, there is a tremendous increase in time lag.

C. LIFETIME

In the lifetime tests, specimens are added with pulse voltage until the final breakdown. 5 specimens are used in each group of Table I to get a set of statistical lifetime data. Fig. 18 shows the results. Although the lifetime of polyimide film is of a bit variety, in the range from 1 Bar to 0.4 Bar, we can see an overall trending that endurance lifetime decreases with pressure decreasing. This is in accordance with the changing of PD magnitude. When the pressure drops to 0.3 Bar, the statistical lifetime is longer than that under 0.5 and 0.4 Bar, and its average value is even longer than that under 0.7 Bar. Fig. 19 shows the eroded areas of the specimen aged under 1 Bar, 0.4 Bar and 0.3 Bar. For the sake of observing under the same lens, other parts of these aged insulation films are cut off. Under continuous PDs generated by the pulse voltage, polyimide molecules matrix would be degraded gradually. Some of the chemical bonds like C-N-C bond in imide ring and C-H bond

in aromatic ring would be destroyed in advance, and then followed by other stronger bonds [22]. The above mentioned aging process forms an unsmooth low density region of byproducts on the surface of insulation film as seen in Fig. 19. Cavities may exist in these eroded areas. In addition, some byproducts with higher conductivity such as amic acid and nitric acid would be generated, which make surface conductivity of the PD eroded area higher [22]. This increased surface conductivity can help dissipate the surface charge faster. Then, PD number during the first stage of aging process decreases since the surface charge is one of the main sources of initial electron [23]. However, with further PD aging, the roughness of the eroded area with cavities can distort the electric field distribution, making PD stronger and easier to be incepted. The specimen aged under 1 Bar has only a small circle eroded around the contact point. While for the specimens aged under low pressure condition (0.4 and 0.3 Bar), the eroded area is larger and can be divided into inner circle and outer circle. The inner circles of these specimens are rougher than that aged under 1 Bar, which indicate a more serious erosion. It can also be noticed that the outer circle aged under 0.3 Bar is larger than that under 0.4 Bar. This implies the PD expands to larger area though the PD magnitude under 0.3 Bar is relatively lower.

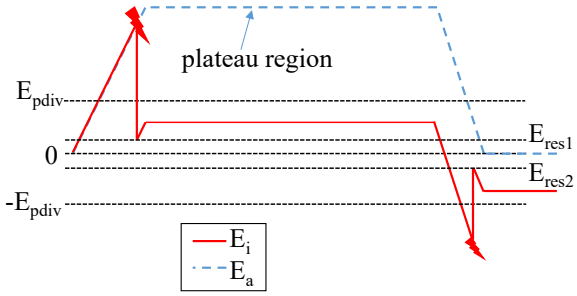

Fig. 15. Changing of the electric filed during the pulse voltage application

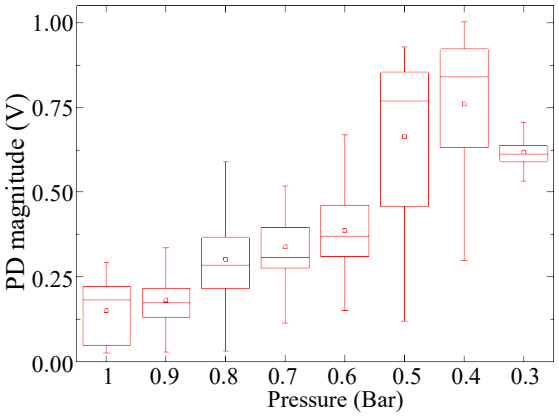

Fig. 16. PD magnitude under different pressures

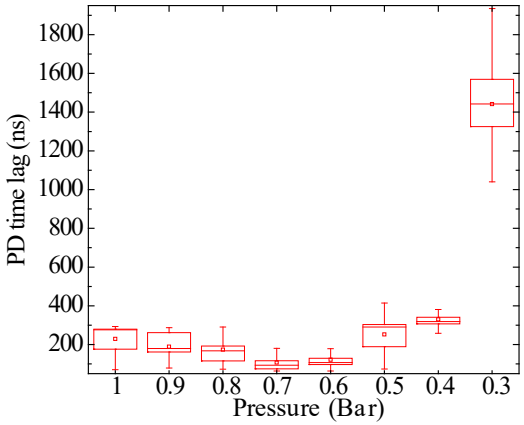

Fig. 17. PD time lag under different pressures

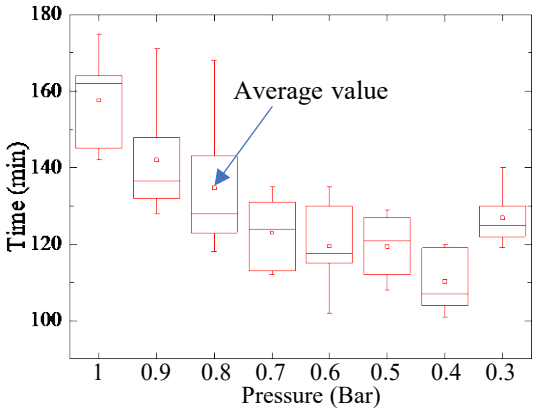

Fig. 18. Endurance lifetime under different pressures

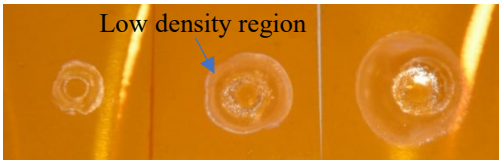

Fig. 19. Eroded area aged under 1 Bar (left), 0.4 Bar (middle) and 0.3 Bar (right)

IV. DISCUSSIONS

In this section, the mechanism of changes of PD features and endurance lifetime with decreasing of pressure would be explained in detail.

A. PD TIME LAG AND MAGNITUDE

For triggering PD, two conditions should be fulfilled, one is that the electrical field strength of the air duct E_i exceeds E_{pdiv}, another is the presence of the initial electron to lead the electron avalanche. So, the total time lag for the PD can be divided into 2 parts expressed by Fig. 20. A time lag t_l should be waited for E_i to reach E_{pdiv} and another statistical time delay Δt is needed for the generation of initial electron and the forming of electron avalanche. If the pressure goes lower, E_{pdiv} decreases, then the E_i can reach E_{pdiv} earlier (t_l decreases). This factor can cause PD happens with a shorter total time lag when pressure decreases in high pressure range (in this case, above 0.7 Bar). Yet, when air pressure decreases, the gas density N is lower, then the number of molecules that can be ionized is reduced. Distance between these molecules is longer and the electron mean free

path increases. This means longer Δt is needed for forming the electron avalanche. Therefore, Δt is increased. Under low pressure range, (in this case, below 0.7 bar), the prolong of electron avalanche plays a dominant role in determining the PD total time lag. When the pressure further drops to 0.4 Bar, the time for forming the avalanche becomes so long that the first and second groups of PDs cannot be triggered under the same electrical stress. So, the time resolved PD pattern under 0.4 Bar in Fig. 13(g) is completely different from that under higher pressures. It is known from the Paschen Curve (seen in Fig. 1) that the breakdown voltage of air duct is affected by air duct length d times pressure p [4]. If d is very short and p is already very low, with further decrease of p, the breakdown voltage of air duct would be raised from the critical point. Therefore, when pressure drops from 0.4 Bar to 0.3 Bar, a part of region 1 (closest to the contact point) in Fig. 6(b) meets an increase in breakdown voltage (corresponds to E_{pdiv} multiplied by d), i.e. the product of p and d in this part of region 1 falls to the left side of the critical point in Pachen's curve. So, PD is less likely to be triggered in this place. However, for the rest regions of the air duct, the product of p and d still lies on the right side of the critical point, which makes PDIV lower when pressure decreases. Meanwhile, compared with that in region 1, the distance of PD in other regions is longer, which can be expressed in Fig. 21. Both the increasing of PD distance and the decreasing number of air molecules prolong the time for forming the electron avalanche, which cause a tremendous increase in PD time lag when pressure drops from 0.4 Bar to 0.3 Bar.

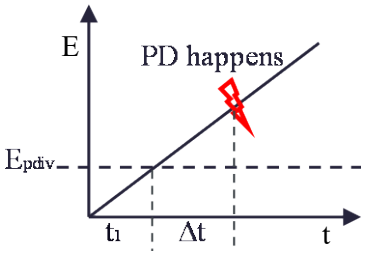

Fig. 20. PD time lag

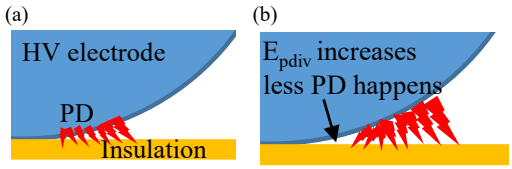

Fig. 21. Main source of PD: (a) Under higher pressures, (b) Under 0.3 Bar

The decreasing of pressure has two effects in the PD intensity. Firstly, if the electric field intensity E keeps unchanged, lower air density N will make E/N higher. E/N is usually used to represent the electron energy [9]. With higher electron energy, stronger PD can be expected with the similar time lag. Secondly, as described in the previous paragraph, under low pressure range, further reducing pressure can make the PD time lag longer. Although there is a segment in the rising edge where voltage drops a little bit (in Fig. 14 where second group of PD happens) and leads to a lower E_i (especially for the PD in region 2 in Fig. 6(b), discussed in section III (b)), in other parts of the rising edge we can still assume that longer PD time lag leads to higher PD firing voltage and higher E_i. In high pressure range (higher than 0.7 Bar), the decreasing of PD time lag and the increasing of electron energy have opposite effects on determining the PD magnitude while the latter plays a dominant role. In low pressure range, the increasing of time lag and increasing of electron energy both enhance the PD intensity. Under 0.3 Bar, PDs mainly happen behind the pulse voltage rising edge and most of them concentrate in time range from 1300 ns to 1600 ns as shown in Fig. 17 and Fig. 22. In this time range, the instantaneous voltage value (from 1.68 kV to 1.82 kV) is obviously lower than the peak value (1.96 kV). Therefore, compared with PDs under 0.4 Bar and the third group of PDs under 0.5 Bar (these PDs mainly happen around the peak point of the pulse voltage, with PD firing voltage usually higher than 1.9 kV), the E_i of the PDs under 0.3 Bar is relatively lower, which leads to lower statistical PD magnitude.

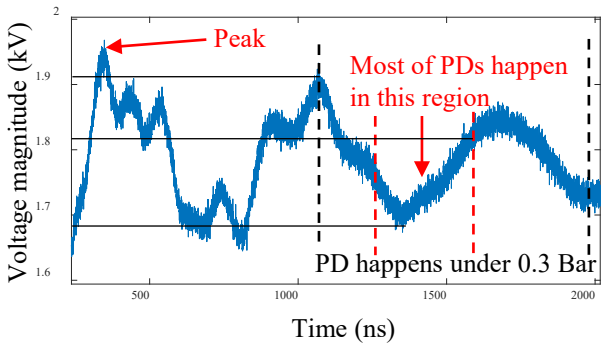

Fig. 22. PD region under 0.3 Bar

B. ENDURANCE

Insulation aging due to PD is a complicated process. PD induced partial temperature rise and chemical reaction will break the molecule chain of the organic insulation material progressively. Among the chemical reaction, intense oxidation is an important factor to degrade the insulation material [22]. With the presence of strong discharge, O_2 molecules can change into O_3 [24], which has stronger oxidability and is more harmful to the organic insulation material. Although higher PD intensity can surely enhance the abovementioned aging factor, when pressure goes lower, O_2 and other compositions in the air that can participate in the insulation aging process become scarcer. Therefore, under low pressure condition, the chemical reaction may be suppressed although the PD activity is still intense, which give rise to a longer lifetime under 0.3 Bar (even longer than that under 0.7 Bar in average).

In this experiment, PD happens in the air duct between sphere electrode and insulation film. If we take both electric field intensity E and pressure p into consideration, for a certain kind of gas dielectric (including air), there is a constant $(E/p)_C$ (represented by a constant C_0 in Fig. 23) to define its breakdown threshold [4]. If the applied (E/p) exceeds C_0 of the air, PD can be triggered in the air duct with the presence of initial electron. Fig. 23 shows the right half of the cross section of the electrodes and insulation sample briefly. For a certain pressure p_1, the value of E/p_1 is a function of the distance L from the contact point, i.e. $E/p_1=f(L)$ as the black curve shows in Fig. 23 [8]. The black curve intersects with the y-axis at point A. With distance shorter than L_1, E/p_1 is higher than C_0. Thus, PD happen in the circle with the contact point as center and L_1 as the radius. If we keep the applied voltage magnitude unchanged and decrease the pressure into p_2, then $E/p_2=f(L)$ is changed into the red curve in

Fig. 23. The curve intersects with y-axis at point B. In this case, PD happen in the circle with the contact point as center and L_2 as the radius. This is the main reason why PD eroded area expands with pressure deceasing.

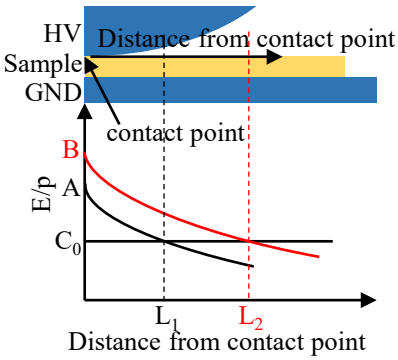

Fig. 23. Expansion of PD area with pressure decreasing

Based on the above studies, we can see that under lower pressures, polyimide film's capability against PD inception and PD aging is obviously weakened. Since this insulation material is usually applied in medium frequency transformers, these experiment results indicate a possible reduction of insulation behavior of medium frequency transformer with pressure decreasing. More into depth studies of actual medium frequency transformer's insulation design are necessary.

V. CONCLUSIONS

To investigate the influence of pressure on PD and its induced aging behavior on the polyimide film, a test system with the abilities of generating pulse voltage, detecting PD, controlling the pressure along with breakdown protection is built. Based on this system, PD (including PDIV and PD features) and endurance tests on the polyimide insulation film under different pressures are conducted. The results show that:

1. PDIV decreases with pressure decreasing under pulse voltage, which fits the right part of Pashen's Curve obtained under sinusoidal voltage.
2. In high pressure range, PD time lag decreases with pressure decreasing because of the reducing partial discharge inception electric field. Yet, with less air molecules, longer time is needed for forming the electron avalanche. When pressure further decreases, PD time lag would be longer due to this factor.
3. With the decreasing of pressure, longer PD time lag (within the voltage rising edge) that leads to higher PD firing voltage and the increasing of electron energy would increase the PD magnitude. Yet, when pressure further decreases, PD would happen behind the voltage rising edge, which give rise to lower PD firing electric field intensity and reduces the PD magnitude.
4. Stronger PD intensity under lower pressure can surely intensify the aging process including the partial temperature rise and chemical reactions and leads to shorter insulation endurance. Yet when pressure continuous decreases, oxygen and other gas molecules in the air that participate in the chemical reaction are greatly reduced, which suppresses the aging process and leads to longer insulation endurance.
5. PD erosion area is larger on the insulation film aged under lower pressure. This is due to that larger area of the air duct exceeds the breakdown threshold when the pressure decreases.

These results show that polyimide insulation film suffer from greater risk of PD inception and deterioration when pressure goes lower and bring focus to the need of more into depth studies of actual medium frequency transformer's insulation design.

REFERENCES

[1] M Mogorovic, "Modeling and Design Optimization of Medium Frequency Transformers for Medium-Voltage High-Power Converters," Phd dissertation, Power Electronics Laboratory., Swiss federal Institute of Technology in Lausanne, Lausanne, 2019.
[2] D. Fabiani, G. C. Montanari, A. Cavallini, and G. Mazzanti, "Relation between space charge accumulation and partial discharge activity in enameled wires under PWM-like voltage waveforms," IEEE Trans. Dielectr. Electr. Insul., Vol. 11, no.3, pp. 393-405, October. 2004.
[3] E. Sili, J. P. Cambronne, N. Naude, R. Khazaka, "Polyimide lifetime under partial discharge aging: effects of temperature, pressure and humidity," IEEE Trans. Dielectr. Electr. Insul., vol. 20, no. 2, pp. 435-442, May. 2013.
[4] High voltage engineering, Butterworth-Heinemann, 2nd ed., Oxford, UK, 2000
[5] S. Jean, B. Reda, M. Xavier, M. Philippe, M. Arnaud, G. Stephane, B. Taoufik, "Planar Magnetic Components in More Electric Aircraft: Review of Technology and Key Parameters for DC–DC Power Electronic Converter," IEEE Transactions on Transportation Electrification., Vol. 3, no. 4, pp. 831-842.
[6] D. James, I. Sauers, A. Elis, M. Pace and D. Deschenes, "Effect of gas pressure on partial discharge in voids in epoxy," Annual Report Conference on Electrical Insulation and Dielectric Phenomena, Albuquerque, NM, USA, October, 2003.
[7] M. Kamarol, S. Ohtsuka, M. Hikita, H. Saitou, M. Sakaki, "Determination of Gas Pressure in Vacuum Interrupter Based on Partial Discharge," IEEE Trans. Dielectr. Electr. Insul., Vol. 14, No. 3, pp. 593-599, 2007.
[8] H. Okubo, S. Yuasa, K. Ota, N. Hayakawa, M. Hikita, "Discharge Characteristics under Non-uniform Electric Field in He, Ar and Air at Low Pressures," IEEE Transactions on Dielectrics and Electrical Insulation., Vol. 4, No. 4, pp. 450-455, 1997
[9] H. Liu, R. Liao, X. Zhao and Y. Lin, "The effect of air pressure on the surface electric field intensity characteristics under negative DC corona discharge in a corona cage," Electrical Power and Energy Systems., Vol. 113, pp. 244-250, 2019
[10] Y. Nakano, M. Kozako, T. Tanaka, M. Kobayashi, "Estimation of Internal Pressure of Vacuum Interrupter by Measuring Partial Discharge Current," IEEE International Symposium on Discharges and Electrical Insulation in Vacuum, Greifswald, Germany, September. 2018, pp. 611-614.
[11] B. Moein and G. Mona,"Characterization of Partial Discharge Activities in WBG Power Converters under Low-Pressure Condition,"Energies., Vol. 14, No. 5394, 2021.
[12] E. Christopher, L. Robert, C. Lan, R. Simon and F. Robert, "The Effects of Pressure and Temperature on Partial Discharge Degradation of Silicone Conformal Coatings," IEEE Trans. Dielectr. Electr. Insul., Vol. 24, No. 5, pp. 2986-2994, 2017.
[13] N. S. Ali, S. Saeed, S. Greg, K. Behzad, "Investigation of Corona Partial Discharge Characteristics under Variable Frequency and Air Pressure," IEEE Electrical Insulation Conference, San Antonio, TX, USA, June. 2018, pp. 31-34
[14] A. Cedric, B. Thibaut, L. Thierry, "Influence of pressure on partial discharge spectra," IEEE Electrical Insulation Conference, Montreal, QC, Canada, June. 2016, pp. 507-510.
[15] D. R. Meyer, A. Cavallini, L. Lusuardi, D. Barater, G. Pietrini, A. Soldati, "Influence of Impulse Voltage Repetition Frequency on RPDIV in Partial Vacuum," IEEE Trans. Dielectr. Electr. Insul., Vol. 25, No. 3, pp. 873-882, 2018.
[16] B. Moein, G. Mona, "A Finite Element Analysis Model for Partial Discharges in Silicone Gel under a High Slew Rate, High Frequency Square Wave Voltage in Low-Pressure Conditions," Energies., Vol. 13, No. 9, 2020.
[17] A. A. Abdelmalik, A. Nysveen and L. Lundgaard,"Influence of Fast Rise Voltage and Pressure on Partial Discharges in Liquid Embedded Power

Electronics," IEEE Trans. Dielectr. Electr. Insul., Vol. 22, No. 5, pp. 2770-2778, 2015.

[18] Y. Zhao, G. Zhang and R. Guo, "The Breakdown Characteristics of Thermostable Insulation Materials under High-Frequency Square Waveform," IEEE Trans. Dielectr. Electr. Insul., vol. 26, no. 4, pp. 1073–1080, 2019.

[19] W. Y. Zhou, P. Wang, Z. J. Zhao, Q. Wu, and A. Cavallini, "Design of an Archimedes spiral antenna for PD tests under repetitive impulsive voltages with fast rise times," IEEE Trans. Dielectr. Electr. Insul., Vol. 26, no. 2, pp. 423–430, March. 2019

[20] P. Wang, H. Xu, J. Wang and W. Wang, "Effect of Repetitive Impulsive Voltage Duty Cycle on Partial Discharge Features and Insulation Endurance of Enameled Wires for Inverter-fed Low Voltage Machines," IEEE Trans. Dielectr. Electr. Insul., Vol. 24, No. 4, pp. 2123-2131, 2017.

[21] L. Niemeyer,"A generalized approach to partial discharge modeling," IEEE Trans. Dielectr. Electr. Insul., Vol.2, No. 4, pp. 510-528, 1995.

[22] X. Zhong, G. Wu, Y. Yang, X. Wu, Y. Lei, "Effects of nanoparticles on reducing partial discharge induced degradation of polyimide/Al2O3 nanocomposites," IEEE Transactions on Dielectrics and Electrical Insulation., Vol. 25, No. 2, pp. 594-602.

[23] Y. Luo, G. Wu, J. Liu, G. Zhu, P. Wang, P, Jia and K. Cao,"PD Characteristics and Microscopic Analysis of Polyimide Film Used as Turn Insulation in Inverter-fed Motor," IEEE Trans. Dielectr. Electr. Insul., Vol. 21, No. 5, pp. 2237-2244, 2014.

[24] P. Yao, H. Zheng, X. Yao, Z. DING, "A Method of Monitoring Partial Discharge in Switchgear Based on Ozone Concentration," IEEE transactions on plasma science., Vol. 47, No. 1, pp. 654-660, 2019.

[25] T. Liu, Q. M. Li, G. J. Dong, M. Asif, X. W. Huang, Z. D. Wan, "Multi-factor model for lifetime prediction of polymers used as insulation material in high frequency electrical equipment," Polym. Test., vol. 73, pp. 193–199, November. 2018.